Citation Information: 10.1016/j.segan.2022.100753

Distributed Methodology for Reactive Power Support of Transmission System

Georgios C. Kryonidis, Maria E. Tsampouri, Kyriaki-Nefeli D. Malamaki, and Charis S. Demoulias

***Abstract*—This paper deals with the provision of reactive power support from distribution grids to the transmission system. To this end, a new distributed control scheme is proposed that coordinates the reactive power output of distributed generation (DG) units to meet a predefined reactive power set-point at the point of interconnection of the distribution grid with the transmission system. The coordination process is implemented in an optimal way minimizing the network losses, while also satisfying the technical limits of the distribution grid. Furthermore, the proposed distributed control scheme is supplemented with a new control algorithm for the on-load tap changer (OLTC) of the high-/medium-voltage transformer to unlock additional reactive power flexibility in case the voltage limits at the distribution grid are reached. Time-series simulations on the IEEE 33-bus network are performed to evaluate the performance of the proposed method against existing solutions.**

***Index Terms*—Distributed algorithm, distributed generation, loss reduction, reactive power support, voltage control.**

I. Introduction

Traditionally, distribution grids were treated by the transmission system operators (TSOs) as passive elements without being actively involved in the control process. Nevertheless, the advent of distributed generation (DG) brought new control and monitoring functionalities, enabling their active participation at the transmission system operation [1]. This is also reflected in the demand connection code published by ENTSO-E, which introduces a closer cooperation between distribution system operators (DSOs) and TSOs to tackle new operational challenges raised by the gradual replacement of large-scale power plants with DG units [2].

Focusing on the provision of reactive power support (RPS), the authors in [3] demonstrated that the available reactive power of DG units can be used instead of the conventional compensation devices to effectively regulate the reactive power at the TSO-DSO interface. This solution has been recently assessed from an economical perspective in [4], where the findings indicated that it can be a viable solution against the use of conventional compensation devices. Furthermore, the performance of the well-established $Q(V)$ and $Q(P)$ droop control schemes is investigated in [5] and [6], respectively, in terms of providing RPS. Nevertheless, a decentralized implementation is assumed for these methods, where control actions are individually performed by each DG unit based only on local measurements. As a result, the reactive power at the TSO-DSO interface cannot be accurately controlled, since DG units operate in an uncoordinated way.

To overcome this limitation, a central controller is introduced in [7] to coordinate the decentralized operation of DG units equipped with $Q(V)$ droop control. The concept of the central controller is also adopted in [8], which is used to adjust the operating set-points of the DG units to meet a predefined power exchange at the TSO-DSO interface. A similar approach is proposed in [9], where an optimization-based solution is presented to optimally dispatch the DG units. In [10], a model-free coordination scheme is proposed to transform the distribution feeder into a controllable PV bus. More specifically, the reactive power of the distribution grid is automatically adjusted to regulate the voltage at the transmission system. Furthermore, a comprehensive framework is proposed in [11] that utilizes phasor measurement units as the main communication mean for the provision of RPS from distribution grid to the transmission system. Finally, the concept of the virtual power plant is proposed in [12] that coordinates DG units located in different geographical areas to provide RPS. Although the above-mentioned methods can effectively provide RPS to the transmission system, their impact on the performance of the distribution grid is not considered.

This drawback can be addressed by integrating additional constraints in the formulation of the optimization problem that model the behavior of the distribution grids, as proposed by the authors in [13] and [14]. However, a linearized network model is assumed which may introduce inaccuracies and infeasible operating points during the real-time grid operation. The full nonlinear network model is considered in the optimization-based methods proposed in [15]–[17]. Scope of these methods is to regulate the reactive power exchange at the TSO-DSO interface with minimum network losses, while also satisfying the technical limits of the distribution grid. Nevertheless, centralized methods suffer from single-point failures due to the use of a central controller. Additionally, these methods use generation and consumption forecasts to determine the operating set-points of DG units. Thus, in case of forecast errors, miscalculations may occur leading to suboptimal and infeasible solutions. Finally, a complete knowledge of the network parameters and operating conditions is needed, limiting their applicability under real-field conditions.

This paper builds on [18] by developing a new distributed control scheme for the provision of RPS at the TSO-DSO interface. Scope of the proposed method is to optimally coordinate the reactive power output of DG units to achieve a predefined RPS set-point without violating the technical constraints

The Authors are with the School of Electrical and Computer Engineering, Aristotle University of Thessaloniki, Thessaloniki GR 54124, Greece (e-mail: kryonidi@ece.auth.gr; tsamp.m@gmail.com; kyriaki_nefeli@hotmail.com; chdimoul@auth.gr). *(Corresponding author: Georgios C. Kryonidis.)*

of the distribution grid. The optimization process targets at the minimization of network losses. The distinct feature of the proposed method lies on the use of a data-driven distributed control architecture, avoiding the use of forecasts and the adverse effects caused by single-point failures. Furthermore, contrary to the centralized methods, the proposed approach requires limited information, thus allowing its implementation under real-field conditions. Finally, a new control algorithm for the on-load tap changer (OLTC) of the high-/medium-voltage (HV/MV) transformer is proposed acting supplementary to the distributed control scheme. The proposed algorithm aims to facilitate the RPS provision in case the voltage limits at the distribution grid are reached.

The rest of the paper is organized as follows: The problem formulation is analytically presented in Section II followed by an overview of the centralized control schemes in Section III. The proposed methodology, i.e., the distributed methodology for RPS supplemented with a new OLTC control algorithm, is presented in Section IV. Simulation results for a radial MV network are presented in Section V and, finally, Section VI concludes the paper.

II. Problem Formulation

The optimal provision of RPS at the TSO-DSO interface constitutes an optimization problem that is mathematically formulated using (1)-(11). More specifically, (1) is introduced as the objective function aiming to minimize the network losses.

$$\min \sum_{i\in N}\sum_{j\in N}\left[\alpha_{ij}\left(p_i p_j + q_i q_j\right)\beta_{ij}\left(q_i p_j - p_i q_j\right)\right] \quad (1)$$

Eq. (1) is the exact loss formula as presented in [19]. N is the set of network nodes, while α_{ij} and β_{ij} are two coefficients calculated by:

$$\alpha_{ij} = \frac{R_{ij}}{V_i V_j} cos(\theta_i - \theta_j) \quad (2)$$

$$\beta_{ij} = \frac{R_{ij}}{V_i V_j} sin(\theta_i - \theta_j) \quad (3)$$

where V_i and θ_i denote the magnitude and angle of the voltage at node i, while R_{ij} is the real part of the ij-th element of the Z-matrix, which is the inverse of the network admittance matrix. Furthermore, in (1), p_i and q_i stand for the net injected active and reactive power at node i calculated according to

$$p_i = \sum_{j\in N} P_{ij} = p_{\mathrm{g},i} - p_{\mathrm{c},i} \quad (4)$$

$$q_i = \sum_{j\in N} Q_{ij} = q_{\mathrm{g},i} - q_{\mathrm{c},i}. \quad (5)$$

Here, $p_{\mathrm{c},i}$ and $q_{\mathrm{c},i}$ are the active and reactive power of the load connected to node i, respectively, whereas $p_{\mathrm{g},i}$ stands for the active power of the DG unit located at node i. Finally, $q_{\mathrm{g},i}$ is the main control variable denoting the reactive power used by the DG unit located at node i, where a positive value indicates a leading power factor, i.e., the DG unit operates in overexcited mode producing reactive power.

The model of the distribution grid is included in the optimization problem using (6) and (7) that represent the active and reactive power flowing through the network branches.

$$P_{ij} = V_i V_j [G_{ij}\cos(\theta_i - \theta_j) + B_{ij}\sin(\theta_i - \theta_j)] \quad (6)$$

$$Q_{ij} = V_i V_j [G_{ij}\sin(\theta_i - \theta_j) - B_{ij}\cos(\theta_i - \theta_j)] \quad (7)$$

P_{ij} and Q_{ij} are the active and reactive power flowing from node i to the directly connected node j. Furthermore, G_{ij} and B_{ij} are the real and imaginary part of the ij-th element of the positive-sequence network admittance matrix.

The concept of the slack bus is introduced to model the transmission system. In particular, the transmission system is modeled as an ideal voltage source where the voltage angle is zero while the voltage magnitude (V_s) is calculated as follows:

$$V_s = V_{\mathrm{hv}}/[m(1+\beta tap)] \quad (8)$$

where V_{hv} stands for the voltage magnitude of the HV network, tap denotes the tap position, β is the variation of the transformation ratio, and m is the nominal transformation ratio. Eq. (8) is introduced to model the OLTC operation of the HV/MV transformer. It is worth mentioning that tap is treated as an input parameter in the optimization problem determining the voltage at the slack bus (V_s).

The provision of RPS at the TSO-DSO interface is incorporated in the optimization problem by adding the following equality constraint:

$$Q_{\mathrm{set}} = \sum_{j\in N} Q_{sj} \quad (9)$$

where Q_{set} is the reference value and Q_{sj} is the reactive power flowing from the slack bus (s) to the directly connected node j. Finally, (10) and (11) are used to model the reactive power capability of DG units and the technical constraints of the distribution grid, respectively.

$$q_{\min,i} \le q_{\mathrm{g},i} \le q_{\max,i} \quad (10)$$

$$V_{\min} \le V_i \le V_{\max} \quad (11)$$

$q_{\min,i}$ and $q_{\max,i}$ are the minimum and maximum reactive power limits of the DG unit connected to node i, which are calculated following the procedure described in [20]. In case no DG unit is connected at node i, the corresponding reactive power limits are set equal to zero. Finally, $V_{\max}$ and $V_{\min}$ are the maximum and minimum permissible voltage limits.

III. Centralized Control Scheme

The optimal RPS provision at the TSO-DSO interface can be implemented by adopting the centralized approach depicted in Fig. 1. More specifically, a central controller is applied to solve the optimization problem of (1)-(11) using the following input data: (a) network configuration, (b) short-term generation and consumption forecasts, and (c) Q_{set}. The output data are the reactive power set-points which are forwarded to the DG units via an ICT infrastructure. This process is repeated at a regular basis, e.g., every 15 min. It is worth mentioning that between two consecutive solutions of the optimization

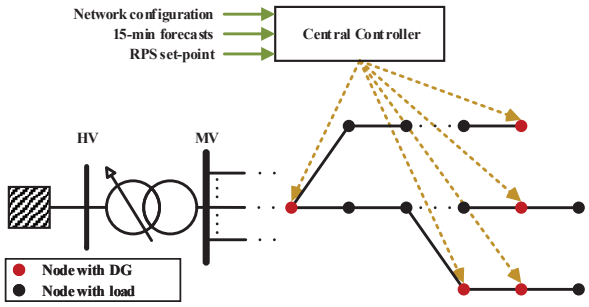

Fig. 1. Conceptual design of the centralized control scheme.

problem, the reactive power output of each DG unit remains constant and equal to the last acquired value. As a result, in case of forecast errors, inaccuracies may occur, increasing also the possibility of voltage violations. Furthermore, the optimization problem of (1)-(11) requires a complete knowledge of the network parameters and operating conditions at each time instant, while single-point failures, e.g. central controller failure, cannot be effectively addressed.

IV. Proposed Method

Scope of the proposed method is to solve the optimization problem as expressed by (1)-(11) following a distributed approach. More specifically, the reactive power of each DG unit is updated by combining local measurements at the point of interconnection with the distribution grid with the information received by neighboring units. Additionally, the proposed distributed control scheme is supplemented with an OLTC algorithm that contributes to the provision of RPS in case the voltage limits at the distribution grid are reached. An analytical description of the developed control strategy is carried out in the next subsections.

A. Distribution Network Modeling

To facilitate the derivation of the update process, the linearized DistFlow model is adopted [21]. In particular, assuming the single branch of Fig. 2, the voltage at node i is calculated as follows:

$$\bar{V}_i = \bar{V}_{\pi i} - \bar{Z}_i \bar{I}_i \tag{12}$$

where $\bar{V}_i$ and $\bar{V}_{\pi i}$ are the complex voltage at node i and its parent node. Furthermore, $\bar{Z}_i$ and $\bar{I}_i$ are the impedance and the current flowing through the line. By multiplying both sides of (12) by the conjugate of $\bar{V}_i$, (13) is derived.

$$V_i^2 = V_{\pi i}^2 - 2\mathrm{Re}\left[\bar{V}_{\pi i}\bar{Z}_i^* \bar{I}_i^*\right] + \left(\bar{Z}_i \bar{I}_i\right)\left(\bar{Z}_i \bar{I}_i\right)^* \tag{13}$$

Here, the last term on the right-hand side is relatively small and can be neglected [21]. Moreover, the apparent power ($\bar{S}_i$) flowing through the line is calculated according to

$$\bar{S}_i = \bar{V}_{\pi i}\bar{I}_i^*. \tag{14}$$

By replacing, (14) to (13), (15) is obtained.

$$V_i^2 = V_{\pi i}^2 - 2\mathrm{Re}\left[\bar{Z}_i^* \bar{S}_i\right] \tag{15}$$

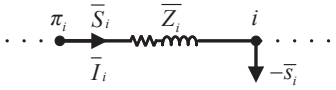

Fig. 2. Single branch.

The power flow balance at node i is calculated as follows:

$$\bar{S}_i - \bar{Z}_i \bar{I}_i \bar{I}_i^* - \sum_{j \in C_i} \bar{S}_j = -\bar{s}_i \tag{16}$$

where $\bar{s}_i$ stands for the injected apparent power at node i and C_i stands for the set of the child nodes of node i. The second term at the left-hand side of (16) models the line losses and can be neglected since they constitute a small part of the power flowing through the line. As a result, (16) is transformed to (17).

$$\bar{S}_i - \sum_{j \in C_i} \bar{S}_j = -\bar{s}_i \tag{17}$$

The linearized DistFlow model as expressed by (15) and (17) can be written in compact form using (18) and (19), respectively.

$$\mathbf{v} = \mathbf{R}\mathbf{p} + \mathbf{X}\mathbf{q} + v_0 \mathbf{1_N} \tag{18}$$

$$\bar{\mathbf{S}} = \mathbf{M}\bar{\mathbf{s}} \tag{19}$$

Here, $\mathbf{v}$ is the Nx1 vector of the square voltages and v_0 is the square voltage of the slack bus. Moreover, $\bar{\mathbf{S}}$ and $\bar{\mathbf{s}}$ denote the Nx1 vectors of the apparent power flowing though the network lines and injected to the network nodes, respectively. $\mathbf{M}$ is equal to $\mathbf{A}^{-\mathrm{T}}$ where $\mathbf{A}$ is the incidence matrix of the network with a size of NxN. Furthermore, $\mathbf{p}$ and $\mathbf{q}$ are the real and imaginary part of $\bar{\mathbf{s}}$, while $\mathbf{R}$ and $\mathbf{X}$ are equal to $2\mathbf{M}^{\mathrm{T}}\mathrm{diag}(\mathrm{Re}\,[\bar{\mathbf{z}}])\mathbf{M}$ and $2\mathbf{M}^{\mathrm{T}}\mathrm{diag}(\mathrm{Im}\,[\bar{\mathbf{z}}])\mathbf{M}$, respectively. Finally, $\mathbf{1_N}$ is the unity vector of size Nx1.

By adopting a similar approach, the line loss for the given single branch of Fig. 2 is calculated according to (20).

$$P_i^{loss} = \mathrm{Re}\left[\bar{Z}_i \bar{I}_i \bar{I}_i^*\right] \tag{20}$$

Assuming that the network voltages are kept close to 1 p.u. [21], (20) is transformed to (21).

$$P_i^{loss} = r_i \bar{S}_i \bar{S}_i^* \tag{21}$$

Therefore, the overall network losses are calculated as follows:

$$\mathbf{P^{loss}} = \mathbf{p}^{\mathrm{T}}\mathbf{R}^{+}\mathbf{p} + \mathbf{q}^{\mathrm{T}}\mathbf{R}^{+}\mathbf{q} \tag{22}$$

where $\mathbf{R}^{+} = \mathbf{M}^{\mathrm{T}}\mathbf{r}\mathbf{M}$ and $\mathbf{r} = \mathrm{diag}(\mathrm{Re}\,[\bar{\mathbf{z}}])$.

B. Distributed Control Scheme for Optimal RPS

The mathematical formulation of the optimization problem that is solved by the proposed distributed control scheme is presented below:

$$\min \mathbf{q}^{\mathrm{T}}\mathbf{R}^{+}\mathbf{q} \tag{23}$$

s.t. (18), (19), and

$$Q_{\mathrm{set}} = Q_{\mathrm{TD}} = -\mathbf{1_N^{\mathrm{T}}}\mathbf{q} \tag{24}$$

$$\mathbf{v}_{\min} \le \mathbf{v} \le \mathbf{v}_{\max} \tag{25}$$

$$\mathbf{q}_{\min} \le \mathbf{q} \le \mathbf{q}_{\max} \tag{26}$$

Eq. (23) is the objective function aiming to minimize the network losses which, according to (22), depend on the active ($\mathbf{p}$) and reactive power ($\mathbf{q}$) injected at the network nodes. Nevertheless, since this paper deals with the provision of reactive power at the TSO-DSO interface, only the impact of the reactive power on the network losses is considered. Furthermore, Q_{TD} is the reactive power flowing at the TSO-DSO interface. Finally, $\mathbf{v}_{\min}$, $\mathbf{v}_{\max}$, $\mathbf{q}_{\min}$, and $\mathbf{q}_{\max}$ stand for the minimum and maximum permissible limits of the network voltages and the reactive power injected at each network node.

The method of Lagrange multipliers is proposed to solve the optimization problem of (23)-(26) [22]. More specifically, the Lagrangian is calculated according to

$$\begin{aligned} L = {} & \mathbf{q}^{\text{T}}\mathbf{R}^{+}\mathbf{q} + \boldsymbol{\mu}^{\mathbf{l}^{\text{T}}}(\mathbf{v}_{\min} - \mathbf{R}\mathbf{p} - \mathbf{X}\mathbf{q} - v_0\mathbf{1}_{\mathbf{N}}) \\ & + \boldsymbol{\mu}^{\mathbf{u}^{\text{T}}}(\mathbf{R}\mathbf{p} + \mathbf{X}\mathbf{q} + v_0\mathbf{1}_{\mathbf{N}} - \mathbf{v}_{\max}) + \boldsymbol{\omega}^{\mathbf{l}^{\text{T}}}(\mathbf{q}_{\min} - \mathbf{q}) \\ & + \boldsymbol{\omega}^{\mathbf{u}^{\text{T}}}(\mathbf{q} - \mathbf{q}_{\max}) + \nu\left(Q_{\text{set}} + \mathbf{1}_{\mathbf{N}}^{\text{T}}\mathbf{q}\right) \end{aligned} \tag{27}$$

$\boldsymbol{\mu}^{\mathbf{l}}$, $\boldsymbol{\mu}^{\mathbf{u}}$, $\boldsymbol{\omega}^{\mathbf{l}}$, and $\boldsymbol{\omega}^{\mathbf{u}}$ are the Lagrangian multipliers associated with the inequality constraints, i.e., (25) and (26), whereas ν is the Lagrangian multiplier related to the equality constraint as expressed by (24). Assuming $\frac{\partial L}{\partial \mathbf{q}} = 0$, (28) is obtained.

$$2\mathbf{R}^{+}\mathbf{q} - \mathbf{X}^{\text{T}}\boldsymbol{\mu}^{\mathbf{l}} + \mathbf{X}^{\text{T}}\boldsymbol{\mu}^{\mathbf{u}} - \boldsymbol{\omega}^{\mathbf{l}} + \boldsymbol{\omega}^{\mathbf{u}} + \boldsymbol{\nu} = 0 \tag{28}$$

In (28), $\mathbf{q}$ includes the reactive power of both DG units ($\mathbf{q_g}$) and loads ($\mathbf{q_c}$) with the latter being uncontrollable. Thus, to move from $\mathbf{q}$ to $\mathbf{q_g}$, (28) is transformed to (29).

$$\mathbf{q_g} = -\mathbf{q_c} + 0.5\mathbf{r}^{-1}\left[-2\mathbf{K}\mathbf{r}\mathbf{Q} + \mathbf{X}^{\text{T}}\boldsymbol{\mu}^{\mathbf{l}} - \mathbf{X}^{\text{T}}\boldsymbol{\mu}^{\mathbf{u}} + \boldsymbol{\omega}^{\mathbf{l}} - \boldsymbol{\omega}^{\mathbf{u}} + \boldsymbol{\nu}\right] \tag{29}$$

Here, $\mathbf{K}$ is equal to $\mathbf{M}^{T} - \text{diag}(\mathbf{1_N})$ and $\mathbf{Q}$ is the imaginary part of $\bar{\mathbf{S}}$. As a result, the reactive power of the DG units ($\mathbf{q_g}(\tau{+}1)$) is updated as follows:

$$\begin{aligned} \mathbf{q_g}(\tau+1) = {} & -\mathbf{q_c}(\tau+1) + 0.5\mathbf{r}^{-1}[-2\mathbf{K}\mathbf{r}\mathbf{Q}(\tau) \\ & + \mathbf{X}^{\text{T}}\boldsymbol{\mu}^{\mathbf{l}}(\tau+1) - \mathbf{X}^{\text{T}}\boldsymbol{\mu}^{\mathbf{u}}(\tau+1) \\ & + \boldsymbol{\omega}^{\mathbf{l}}(\tau+1) - \boldsymbol{\omega}^{\mathbf{u}}(\tau+1) + \boldsymbol{\nu}(\tau+1)] \end{aligned} \tag{30}$$

Furthermore, the updates of the Lagrangian multipliers are determined using (31).

$$\begin{aligned} \boldsymbol{\mu}^{\mathbf{u}}(\tau+1) &= [\boldsymbol{\mu}^{\mathbf{u}}(\tau) + \gamma(\mathbf{v}(\tau) - \mathbf{v}_{\max})]_{+} \\ \boldsymbol{\mu}^{\mathbf{l}}(\tau+1) &= \left[\boldsymbol{\mu}^{\mathbf{l}}(\tau) + \gamma(-\mathbf{v}(\tau) + \mathbf{v}_{\min})\right]_{+} \\ \boldsymbol{\omega}^{\mathbf{u}}(\tau+1) &= \left[\boldsymbol{\omega}^{\mathbf{u}}(\tau) + \delta(\mathbf{q_g}(\tau) - \mathbf{q}_{\max})\right]_{+} \\ \boldsymbol{\omega}^{\mathbf{l}}(\tau+1) &= \left[\boldsymbol{\omega}^{\mathbf{l}}(\tau) + \delta(-\mathbf{q_g}(\tau) + \mathbf{q}_{\min}\right]_{+} \\ \boldsymbol{\nu}(\tau+1) &= \boldsymbol{\nu}(\tau) + \epsilon(Q_{\text{set}} - Q_{\text{TD}}(\tau))\mathbf{1_N} \end{aligned} \tag{31}$$

Here, the operator $[\ ]_{+}$ defines the projection on the positive orthant, whereas γ, δ, and ϵ are positive constant parameters determining the convergence rate. These parameters are case-sensitive depending mainly on the configuration of the examined network and the number of DG units. In this paper, γ and δ are equal to $3 \cdot 10^{-4}$ and $6 \cdot 10^{-2}$, while ϵ is equal to $3.6 \cdot 10^{-3}$.

The proposed control scheme can be implemented under real-field conditions by adopting the configuration presented in Fig. 3. In particular, an ICT infrastructure is used to forward Q_{TD} to the DG units. It is worth mentioning that a synchronous

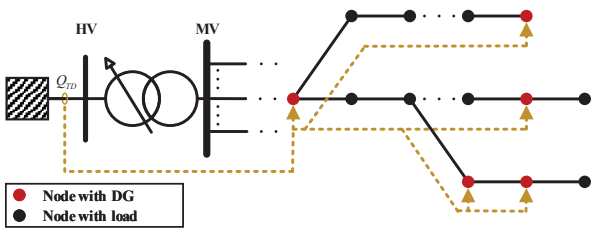

Fig. 3. Conceptual design of the distributed control scheme.

implementation is considered, i.e., the information is provided at the same time in the DG units. Afterward, each DG unit updates locally the Lagrangian multipliers according to (31) by combining local information, i.e., the voltage at the point of interconnection with grid, and information received by the ICT infrastructure, i.e., Q_{TD}, $\mathbf{v}$ and $\mathbf{Q}$. Finally, the updated reactive power output of each DG unit is calculated using (30).

C. OLTC Algorithm

According to the above-mentioned analysis, it can be observed that the regulation of network voltages and the provision of RPS at the TSO-DSO interface may lead to conflicts. For example, for a given time instant t, let us assume that the DG units need to absorb reactive power to tackle overvoltages within the distribution grid. Thus, the reactive power at the TSO-DSO interface will flow from the HV grid to the distribution grid. An attempt to limit the reactive power at the TSO-DSO interface by letting some DG units to inject reactive power would probably lead to overvoltages. Since priority is given to maintaining the network voltages within the permissible limits, the reactive power set-point at the TSO-DSO interface cannot be reached. This problem can be solved by reducing the network voltages, and thus the reactive power absorbed by the DG units, using the OLTC of the HV/MV transformer. Note that after the tap operation, it should be ensured that the network voltages are kept above the minimum limit. The proposed OLTC operation can be expressed mathematically as follows:

$$tap^{t+1} = \begin{cases} tap^{t} + 1, & \text{if } \mathbf{v}^{t+1} > \mathbf{v}_{\min} \text{ and } Q_{\text{TD}}^{t} < Q_{\text{set}}^{t} \\ tap^{t} - 1, & \text{if } \mathbf{v}^{t+1} < \mathbf{v}_{\max} \text{ and } Q_{\text{TD}}^{t} > Q_{\text{set}}^{t} \\ tap^{t}, & \text{otherwise} \end{cases} \tag{32}$$

where $\mathbf{v}^{t}$ denotes the vector of network voltages at time instant t. Assuming a tap change occurs, the network voltages at the next time instant ($\mathbf{v}^{t+1}$) can be estimated by adding a voltage variation ($\Delta\mathbf{v}$). This value refers to the voltage variation per tap change, plus a small value, indicating the small impact of the changing loading conditions.

V. Numerical Results

The performance of the proposed distributed methodology is evaluated by performing time-series simulations on the 12.66 kV MV distribution grid depicted in Fig. 4. Details regarding the network configuration, the line parameters, and the rated power of the loads are presented in [23]. To evaluate the performance of the proposed OLTC algorithm, the examined

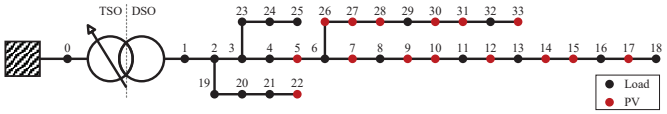

Fig. 4. Topology of the examined MV network.

distribution grid had been modified by including a HV/MV transformer equipped with an OLTC, as shown in Fig. 4. The HV/MV transformer has rated power 50 MVA, short-circuit voltage 12%, whereas the full load losses are 0.5%. The OLTC range is ±8 with a voltage variation of 1.25% per tap. Moreover, 15 PV units are connected to the nodes denoted with red color in Fig. 4 transforming the initially passive grid to active. The nominal power factor of the PV units is equal to 0.8, while their connection node and the corresponding rated power are presented in Table I. Finally, the voltage at the slack bus is kept constant and equal to 1 p.u., while the minimum and maximum voltage limits are 0.95 and 1.05 p.u., respectively.

The simulation period is one day with a time resolution of 1 min. Normalized generation and consumption profiles, similar to those presented in Fig. 5 are arbitrary distributed to the PV units and loads. It is worth mentioning that the power factor of all loads remains constant and equal to the nominal value defined in [23]. Moreover, a zero tap position is assumed for the OLTC for all the simulation period. The proposed method is compared against a centralized, optimization-based method. More specifically, the following scenarios are considered:

- Centralized method without RPS (CN). In this scenario, an optimization-based method is considered where the provision of RPS is neglected. Eqs. (1)-(8) and (10)-(11) are solved at each time instant using the IPOPT solver in GAMS [24].
- Proposed method without RPS (PN). Similar to CN, RPS is deactivated, i.e., $\nu = 0$. In this scenario, two softwares are employed, namely OpenDSS and MATLAB. The former is used as a power flow solver and the latter is employed to implement the iterative process as expressed by (30) and (31) at each time instant. Note that at each iteration, a connection is established between MATLAB and OpenDSS exchanging information, i.e., reactive power set-points and network voltages.
- Centralized method with RPS (CW). This is an enhanced version of the CN including also the provision of RPS. In particular, (1)-(11) are solved at each time instant using the IPOPT solver in GAMS [24].
- Proposed method with RPS (PW). This is the complete version of the proposed methodology, considering also the provision of RPS.

The daily profile of the active and reactive power at the TSO-DSO interface is depicted in Fig. 6, while daily profiles associated with the operating conditions within the distribution grid are presented in Fig 7. In particular, the voltage magnitude at the most remote PV node, i.e., node 17, is illustrated in Fig. 7a. This is the most critical node for overvoltage

TABLE I
RATED ACTIVE POWER OF PV UNITS

Node	MWp	Node	MWp	Node	MWp
5	0.35	7	0.50	9	0.70
10	0.30	12	0.80	14	0.35
15	0.70	17	0.50	22	0.50
26	0.25	27	0.70	28	0.25
30	0.80	31	0.35	33	0.35

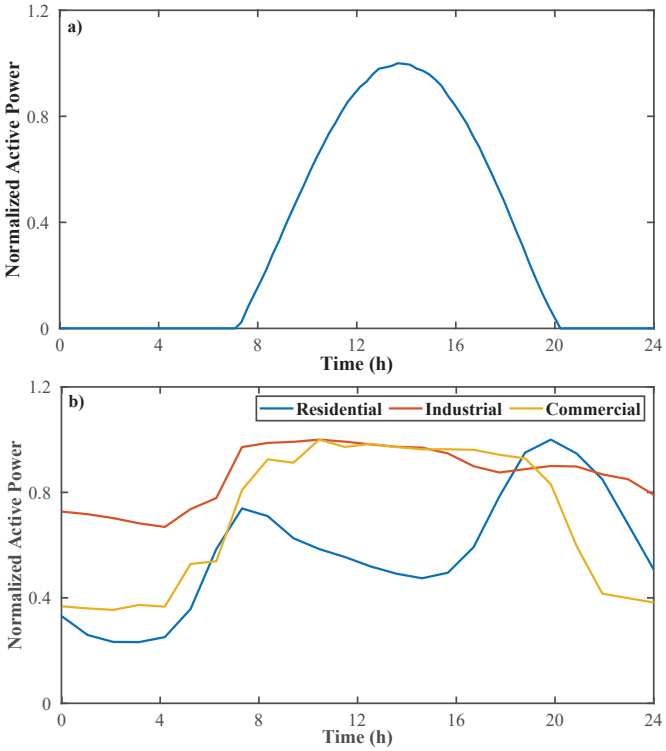

Fig. 5. Daily normalized active power profiles. a) Generation and b) consumption.

mitigation since it presents the maximum network voltage in case no control is applied and PV units operate with unity power factor. The overall reactive power used by the PV units is shown in Fig. 7b. Furthermore, the network losses are presented in Fig. 7c. Finally, the daily reactive energy used by the PV units and the network energy losses are presented in Table II.

According to Fig. 6a, it can be observed that the distribution grid presents an inductive behaviour for all the simulation period in case RPS is neglected. On the contrary, the provision of the RPS actively controls the reactive power at the TSO-DSO interface reaching zero values, i.e., unity power factor. It worth mentioning that both CW and PW can effectively track the reference value at the TSO-DSO interface.

Considering the active power at the TSO-DSO interface, all the examined scenarios lead to a similar profile, as shown in Fig. 6b. Small mismatches are observed for specific time instants which are mainly related to the fact that each examined scenario leads to a different profile of network losses, as verified in Fig. 7c.

Focusing on the operating conditions within the distribution

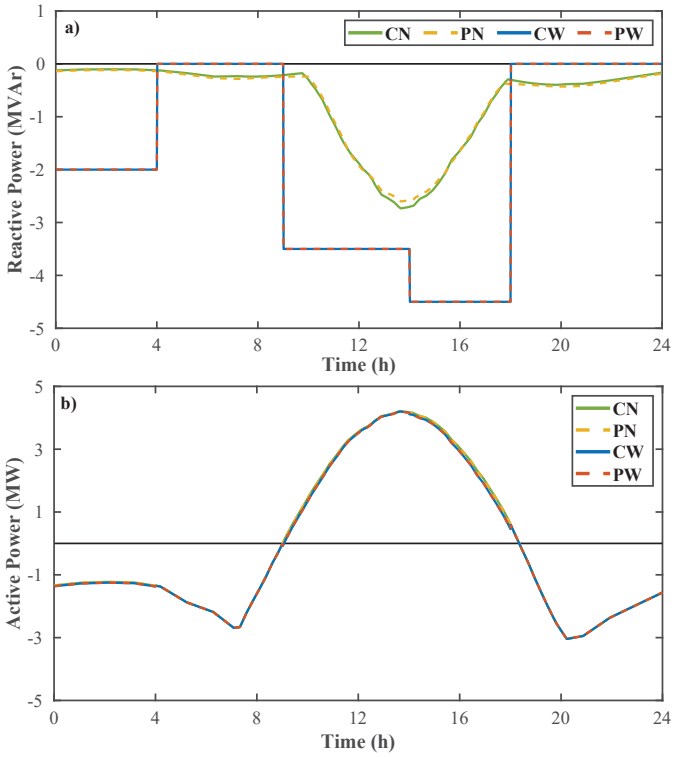

Fig. 6. Daily power profiles at TSO-DSO interface. a) Reactive power and b) active power. Positive sign indicates power flow from MV grid towards the upstream HV grid.

TABLE II
DAILY PV REACTIVE ENERGY AND NETWORK ENERGY LOSSES

	CN	PN	CW	PW
Energy (MVArh)	47.12	50.01	60.27	63.47
Losses (MWh)	3.33	3.35	4.15	4.17

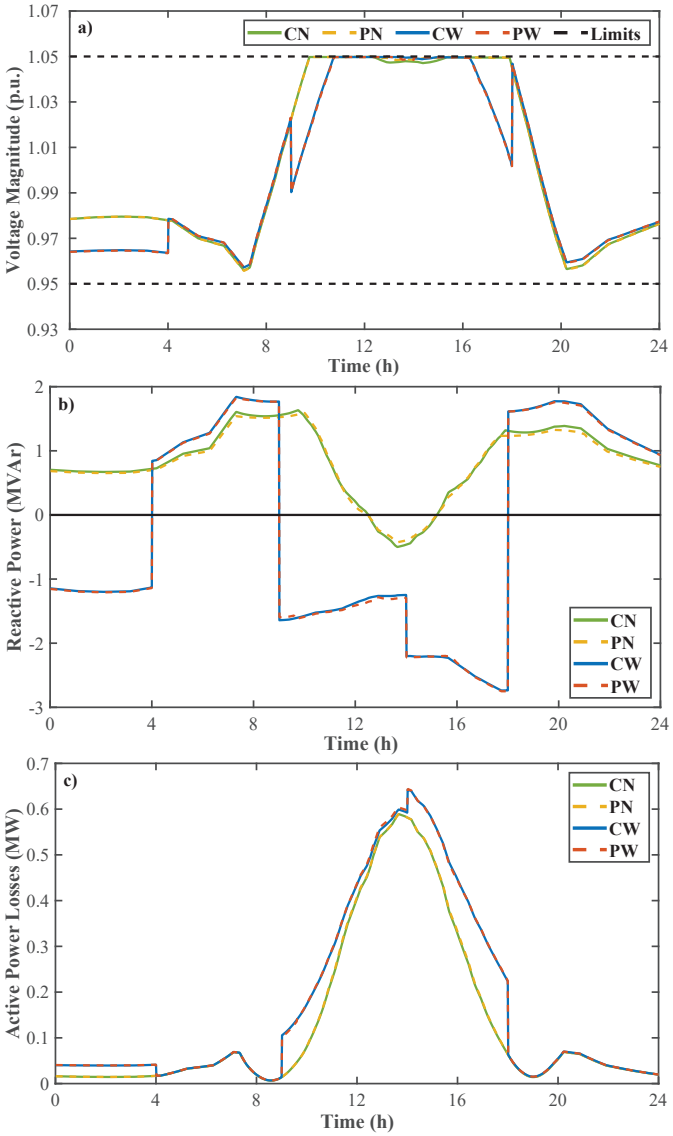

Fig. 7. Daily profiles associated with the distribution grid. a) Voltage magnitude at node 17, b) overall reactive power of PV units, and c) network losses.

grid, it can be concluded that all the examined scenarios can maintain the network voltages within the permissible limits, as shown in Fig. 7a. Additionally, in both implementations, i.e. with and without RPS, the proposed control scheme leads to similar amounts of reactive power compared to the centralized method. This is also evident in Table II where the maximum mismatch is 6.13 %.

In terms of network losses, the proposed method and the centralized control scheme have almost identical power profiles, as shown in Fig. 7c. This can be also verified in Table II where the maximum mismatch is 0.6 %, indicating that the proposed control scheme can achieve near optimal solutions.

To assess the impact of forecast errors on the performance of the centralized, optimization-based solutions, a new series of time-series simulations are performed. This is attained by adopting the following procedure: Initially, the output data of the optimization process, i.e., the reactive power of PV units, are determined every 15 min assuming generation and consumption forecasts. Afterward, the output data are used to perform a power flow analysis for a 15 min timeslot. During this analysis, forecasts errors are applied to the generation and consumption forecasts, varying from 5% to 30%. In this paper, forecast errors are only applied to consumption profiles, since the assumed PV profile is a sunny day that can be accurately predicted. The corresponding results are presented in Fig. 8. It can be observed that the centralized, optimization-based method fails to accurately control the reactive power at the TSO-DSO interface. Additionally, overvoltages occur at the distribution grid, as shown in Fig. 8b. On the contrary, the performance of the proposed method is not affected by the assumed consumption and generation profiles, since it is a data-driven method. As a result, it can effectively control the reactive power at the TSO-DSO interface and ensure that network voltages are kept within the permissible limits.

Finally, the coordinated operation of the OLTC algorithm with the distributed control scheme is assessed in Fig. 9 using the initial daily simulation case. Two scenarios are examined, namely the PW with and without the proposed OLTC algorithm. According to Fig. 9a, it can be observed that when no action is made by the OLTC, the PW fails to regulate

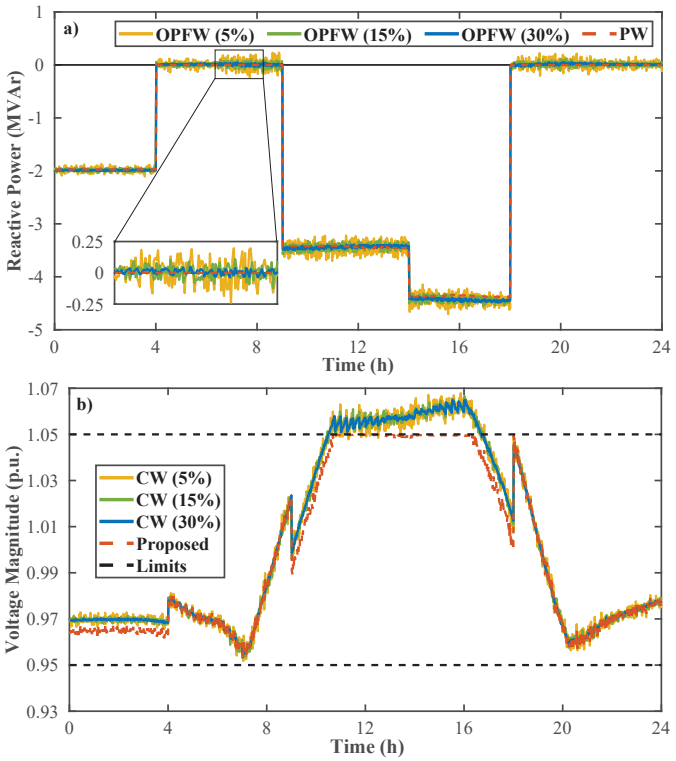

Fig. 8. Impact of forecast errors on the daily profiles. a) Reactive power at TSO-DSO interface and b) voltage magnitude at node 17.

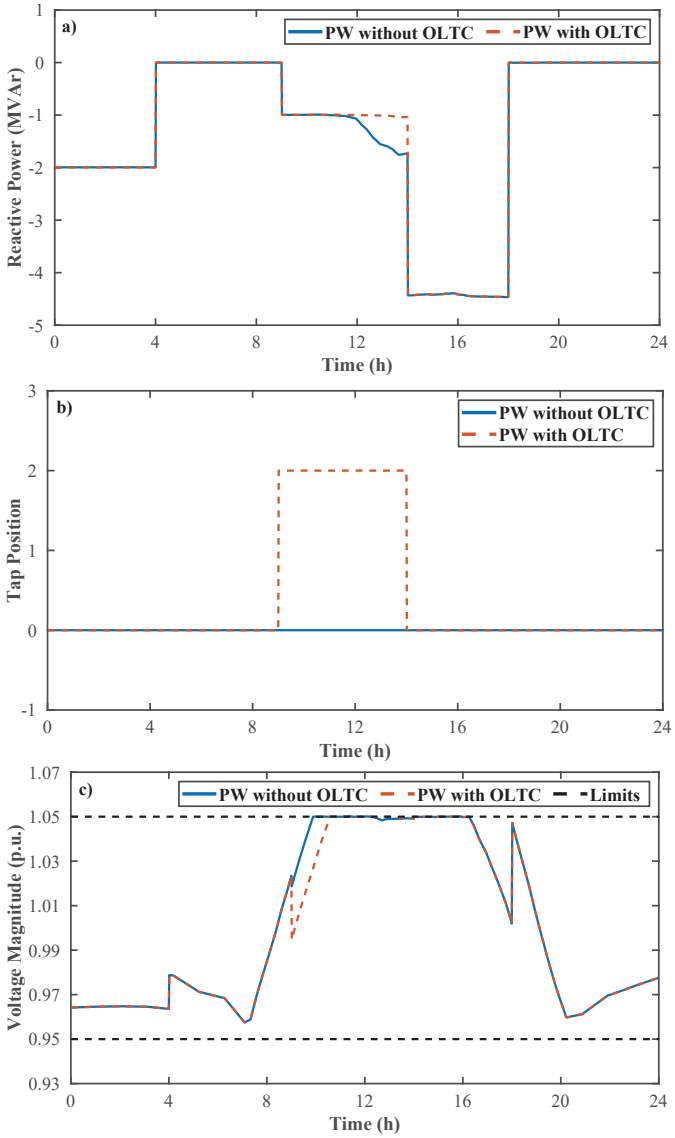

Fig. 9. Daily profiles for the evaluation of the supplementary OLTC algorithm. a) Reactive power at TSO-DSO interface, b) tap position, and c) voltage magnitude at node 17.

the reactive power at the TSO-DSO interface. The main reason lies on the fact that the PV units have reached their maximum reactive power limits by regulating the network voltages. This issue can be effectively addressed using the proposed OLTC algorithm. In particular, according to Fig. 9b, the tap is moved from 0 to 2 to reduce the network voltages. As a result, the overall amount of reactive power needed for voltage regulation is also decreased. Therefore, there exist a sufficient amount of available reactive power to control the reactive power at the TSO-DSO interface, as verified in Fig. 9a.

VI. Conclusions

In this paper, a new data-driven distributed control scheme is proposed for the provision of RPS at the TSO-DSO interface. The proposed method coordinates the reactive power of DG units to achieve a predefined RPS set-point, considering also the technical constraints of the distribution grid. Moreover, a new OLTC algorithm is proposed acting supplementary to the proposed distributed control scheme. The proposed algorithm facilitates the RPS provision in case the voltage limits at the distribution are reached. The validity of the proposed method is demonstrated by performing time-series simulations on a MV distribution grid, highlighting its improved performance compared to centralized methods in terms of robustness to forecast errors. Finally, the proposed method leads to near optimal solutions.

Acknowledgment

This research is co-financed by Greece and the European Union (European Social Fund - ESF) through the Operational Programme "Human Resource Development, Education and Lifelong Learning" in the context of the project "Reinforcement of Postdoctoral Researchers - 2nd Cycle" (MIS-5033021), implemented by the State Scholarships Foundation (IKY).

Ευρωπαϊκή Ένωση
European Social Fund
Operational Programme
Human Resources Development, Education and Lifelong Learning
Co-financed by Greece and the European Union
ΕΣΠΑ 2014-2020

References

[1] S. Karagiannopoulos, J. Gallmann, M. G. Vayá, P. Aristidou, and G. Hug, "Active distribution grids offering ancillary services in islanded and grid-connected mode," *IEEE Trans. Smart Grid*, vol. 11, no. 1, pp. 623–633, 2020.

[2] ENTSO-E, "Demand connection code," *Official J. Eur. Union*, Aug. 2016.

[3] M. Kraiczy, H. Wang, S. Schmidt, F. Wirtz, and M. Braun, "Reactive power management at the transmission–distribution interface with the support of distributed generators – a grid planning approach," *IET Gener., Transm. Distrib.*, vol. 12, no. 22, pp. 5949–5955, 2018.

[4] A. Bachoumis, C. Kaskouras, G. P. Papaioannou, and M. Sousounis, "Tso/dso coordination for voltage regulation on transmission level: A greek case study," in *2021 IEEE Madrid PowerTech*, 2021, pp. 1–7.

[5] Z. Cheng and X. Feng, "A study of DER Volt and Var droop aggregation for reactive power support to transmission system," in *2018 IEEE Power Energy Soc. General Meeting (PESGM)*, 2018, pp. 1–5.

[6] M. Tomaszewski, S. Stanković, I. Leisse, and L. Söder, "Minimization of reactive power exchange at the DSO/TSO interface: Öland case," in *2019 IEEE PES Innov. Smart Grid Technol. Europe (ISGT-Europe)*, 2019, pp. 1–5.

[7] G. Valverde, D. Shchetinin, and G. Hug-Glanzmann, "Coordination of distributed reactive power sources for voltage support of transmission networks," *IEEE Trans. Sustain. Energy*, vol. 10, no. 3, pp. 1544–1553, 2019.

[8] D. M. Gonzalez, L. Robitzky, S. Liemann, U. Häger, J. Myrzik, and C. Rehtanz, "Distribution network control scheme for power flow regulation at the interconnection point between transmission and distribution system," in *2016 IEEE Innov. Smart Grid Technol. - Asia (ISGT-Asia)*, 2016, pp. 23–28.

[9] C. Rodio, G. Giannoccaro, S. Bruno, M. Bronzini, and M. L. Scala, "Optimal dispatch of distributed resources in a tso-dso coordination framework," in *2020 AEIT Int. Ann. Conf. (AEIT)*, 2020, pp. 1–6.

[10] D. B. Arnold, M. D. Sankur, M. Negrete-Pincetic, and D. S. Callaway, "Model-free optimal coordination of distributed energy resources for provisioning transmission-level services," *IEEE Trans. Power Syst.*, vol. 33, no. 1, pp. 817–828, 2018.

[11] A. O. Rousis, D. Tzelepis, Y. Pipelzadeh, G. Strbac, C. D. Booth, and T. C. Green, "Provision of voltage ancillary services through enhanced tso-dso interaction and aggregated distributed energy resources," *IEEE Trans. Sustain. Energy*, vol. 12, no. 2, pp. 897–908, 2021.

[12] J. Ali, S. Massucco, and G. Petretto, "Reactive power provision to tso/dso by aggregators and conventional generators," in *2017 IEEE Int. Conf. Smart Grid Comm. (SmartGridComm)*, 2017, pp. 486–491.

[13] G. Valverde and T. Van Cutsem, "Control of dispersed generation to regulate distribution and support transmission voltages," in *2013 IEEE Grenoble Conf.*, 2013, pp. 1–6.

[14] J. Morin, F. Colas, S. Grenard, J. Dieulot, and X. Guillaud, "Coordinated predictive control in active distribution networks with HV/MV reactive power constraint," in *2016 IEEE PES Innov. Smart Grid Technol. Conf. Europe (ISGT-Europe)*, 2016, pp. 1–6.

[15] K. Tang, R. Fang, L. Wang, J. Li, S. Dong, and Y. Song, "Reactive power provision for voltage support activating flexibility of active distribution networks via a TSO-DSO interactive mechanism," in *2019 IEEE Innov. Smart Grid Technol. - Asia (ISGT Asia)*, 2019, pp. 116–121.

[16] S. Karagiannopoulos, C. Mylonas, P. Aristidou, and G. Hug, "Active distribution grids providing voltage support: The Swiss case," *IEEE Trans. Smart Grid*, article in press.

[17] Y. Yi, X. Chu, and Y. Liu, "Activating reactive power support from active distribution systems," in *2018 IEEE Power Energy Soc. General Meeting (PESGM)*, 2018, pp. 1–5.

[18] G. C. Kryonidis, M. E. Tsampouri, K.-N. D. Malamaki, and C. S. Demoulias, "Distributed methodology for reactive power support of transmission system," in *2021 Int. Conf. Smart Energy Syst. Technol. (SEST)*, 2021, pp. 1–6.

[19] N. Acharya, P. Mahat, and N. Mithulananthan, "An analytical approach for dg allocation in primary distribution network," *Int. J. Electr. Power & Energy Syst.*, vol. 28, no. 10, pp. 669–678, 2006.

[20] G. C. Kryonidis, C. S. Demoulias, and G. K. Papagiannis, "A two-stage solution to the bi-objective optimal voltage regulation problem," *IEEE Trans. Sustain. Energy*, vol. 11, no. 2, pp. 928–937, 2020.

[21] J. Li, C. Liu, M. E. Khodayar, M.-H. Wang, Z. Xu, B. Zhou, and C. Li, "Distributed online var control for unbalanced distribution networks with photovoltaic generation," *IEEE Trans. Smart Grid*, vol. 11, no. 6, pp. 4760–4772, 2020.

[22] Z. Tang, D. J. Hill, and T. Liu, "Distributed coordinated reactive power control for voltage regulation in distribution networks," *IEEE Trans. Smart Grid*, vol. 12, no. 1, pp. 312–323, 2021.

[23] M. E. Baran and F. F. Wu, "Network reconfiguration in distribution systems for loss reduction and load balancing," *IEEE Trans. Power Del.*, vol. 4, no. 2, pp. 1401–1407, 1989.

[24] R. E. Rosenthal, *GAMS: A User's Guide*, GAMS Development Corporation, Washington, DC, USA, 2016.